J. Fluid Mech. (1994), *vol.* 261, *pp.* 253–271

Baroclinic instability of Kirchhoff's elliptic vortex

By TAKESHI MIYAZAKI[1] AND HIDESHI HANAZAKI[2]

[1] Department of Mechanical and Control Engineering, University of Electro-Communications, Chofu, Tokyo 182, Japan

[2] Division of Atmospheric Environment, National Institute for Environmental Studies, Tsukuba, Ibaraki 305, Japan

(Received 19 February 1993 and in revised form 18 August 1993)

The linear instability of Kirchhoff's elliptic vortex in a vertically stratified rotating fluid is investigated using the quasi-geostrophic, f-plane approximation. Any elliptic vortex is shown to be unstable to baroclinic disturbances of azimuthal wavenumber $m = 1$ (bending mode) and $m = 2$ (elliptical deformation). The axial wavenumber of the unstable bending mode approaches $\lambda_c = 1.7046$ in the limit of small ellipticity, indicating that it is a short-wave baroclinic instability. The instability occurs when the bending wave rotates around the vortex axis with angular velocity identical to the rotation rate of the undisturbed elliptic vortex. On the other hand, the wavenumber of the elliptical deformation mode approaches zero in the same limit, showing that it is a long-wave sideband instability.

1. Introduction

A concentrated vorticity region often appears as a coherent structure in geophysical flows, where the fluid motions are subjected to the strong influence both of the Coriolis force and the density inhomogeneity associated with temperature and/or salinity variations. Vertical vortices (which here means those with vertical vorticity component), such as the 'Meddies' in the ocean, keep their identity for a very long time. The motion and stability of these vortices embedded in a stratified rotating fluid is an important aspect of the understanding of the physical mechanisms of energy and momentum transport in geophysical flows.

Geophysical fluid motions are often well described by a quasi-geostrophic approximation (e.g. Pedlosky 1979) and many investigations on vortex instability have been performed based on the quasi-geostrophic, f-plane equations. For instance, Flierl (1988) solved the normal-mode equations analytically for a class of isolated model vortices with piecewise-constant velocity. He showed that a 'baroclinic' instability mode becomes more unstable than barotropic modes, if the scale of the whole vortex is small compared to the radius of deformation. Similarly, Gent & McWilliams (1986) and Carton & McWilliams (1989) solved numerically the normal-modes equations for several continuous vorticity profiles. They reported that the fastest growing perturbation is often 'baroclinic' (they called it an internal instability). The 'baroclinic' instability is sometimes called the 'internal barotropic' instability, but we follow the terminology of Flierl throughout this paper.

The basic flows considered by these previous studies are axisymmetric. Some theoretical results have been given for the stability of circular vortices using conserved quantities such as the energy, the angular momentum and the area enclosed by an isovorticity line. Dritschel (1988*a*) proved the nonlinear (Liapunov) stability of a

vortex patch with uniform vorticity and of vortices with radially monotonically decreasing potential vorticity. Kloosterziel & Carnevale (1992) considered vortices with general vorticity distribution. They constructed a conserved quantity such that the first variation is zero and the second variation is positive or negative definite (formal stability), and showed that the linear barotropic stability regime for a circular vortex coincides with the formal barotropic stability regime. In finite-dimensional systems formal stability implies nonlinear stability whereas in infinite dimensions it is not a necessary prerequisite for nonlinear stability.

We consider the linear stability of an elliptic vortex patch in this paper. Specifically, we consider Kirchhoff's elliptic vortex, a vortex patch with uniform vorticity ω_0 inside an ellipse whose major and minor semi-axes are a and b. If it is embedded in an irrotational fluid, it rotates solidly with a constant angular velocity $\Omega = \omega_0 ab/(a+b)^2$. Love (1893) studied the linear barotropic stability of Kirchhoff's elliptic vortex and showed that it becomes unstable to disturbances with azimuthal wavenumber 3, if the ratio a/b is greater than 3. Meacham (1992) considered the stability of quasi-geostrophic ellipsoidal vortices, extending Love's work. He determined the dispersion relations of normal modes utilizing the expansions in ellipsoidal harmonics (Lame functions). He demonstrated that unstable modes exist over a considerable range of the geometrical parameters that characterize the ellipsoid. In this study, we consider the baroclinic instability of Kirchhoff's elliptic vortex. This may be covered by Meacham's analysis as a limiting case of (his parameters) α, $\beta \to 0$ with α/β being fixed. However, Meacham did not pay special attention to this parameter region and a separate analysis is necessary in order to obtain refined information. To obtain the physical interpretation of the instability, it is helpful that we consider a geometrically less complicated case.

We formulate the eigenvalue problem for normal modes in §2. The perturbation streamfunctions are expanded in terms of the Mathieu functions, since an elliptic vortex is considered. The eigenvalues are determined numerically after truncating the expansions at some finite order. The results of the stability analysis are demonstrated in §3. Any ellipse (irrespective of a/b) is shown to be unstable to baroclinic disturbances with azimuthal wavenumbers $m = 1$ and $m = 2$. In §4, we consider the physical mechanisms of instabilities in the limit of small ellipticity, where the cause of the twisting instability ($m = 1$) is shown to be a resonance between the baroclinic inertial (bending) wave and the barotropic $m = 2$ (elliptical deformation) wave, whereas the $m = 2$ baroclinic instability is thought of as a sideband (Benjamin–Feir) instability. The relation of our results to Dritschel's nonlinear-stability criterion is discussed there. The last section is devoted to summary

2. Formulation

The fluid is assumed to be inviscid, incompressible and stably stratified. Our reference frame is rotating with an angular velocity $\frac{1}{2}f$ about the vertical axis z. The quasi-geostrophic equations of motion (conservation of the potential vorticity: e.g. Pedlosky 1979) on the f-plane are written in terms of a streamfunction ψ as

$$\left[\frac{\partial}{\partial t}+\frac{\partial \psi}{\partial y}\frac{\partial}{\partial x}-\frac{\partial \psi}{\partial x}\frac{\partial}{\partial y}\right][\nabla^2+\mathrm{L}_z]\psi = 0. \tag{1}$$

The Cartesian coordinates (x, y, z) are used with the corresponding unit vectors $\boldsymbol{e}_x$, $\boldsymbol{e}_y$

and $\boldsymbol{e}_z$. Here, $\nabla^2 = \partial^2/\partial x^2 + \partial/\partial y^2$ denotes the Laplacian operator in the horizontal plane, and L_z is a differential operator representing the effect of stratification, given by

$$L_z = \frac{1}{\rho_s}\frac{\partial}{\partial z}\left(\frac{\rho_s}{S}\frac{\partial}{\partial z}\right) \tag{2a}$$

for atmospheric synoptic-scale motions or by

$$L_z = \frac{\partial}{\partial z}\left(\frac{1}{S}\frac{\partial}{\partial z}\right) \tag{2b}$$

for oceanic synoptic-scale motions. Here $\rho_s(z)$ is the density of a 'standard' atmosphere and $S(z)$ is the stratification parameter (see Pedlosky 1979, §6). The explicit form of L_z is not required in the following stability analysis. The streamfunction is here defined by (see Love 1983).,

$$u = \partial\psi/\partial y, \quad v = -\partial\psi/\partial x. \tag{3}$$

The streamfunction inside Kirchhoff's elliptic vortex is given by

$$\Psi_{in} = -(bx^2 + ay^2)/2(a+b), \tag{4}$$

where the uniform (relative) vorticity in the interior of the ellipse is taken to be unity and a is the major semi-axis and b is the minor semi-axis. Kirchhoff's elliptic vortex rotates rigidly about the z-axis with a constant angular velocity

$$\Omega = ab/(a+b)^2. \tag{5}$$

The elliptic-cylinder coordinates (ξ, η, z) are convenient in describing the geometry of the basic flow field:

$$x = c\cosh\xi\cos\eta, \tag{6a}$$

$$y = c\sinh\xi\sin\eta, \quad 0 \leqslant \eta \leqslant 2\pi, \tag{6b}$$

where $c = (a^2 - b^2)^{\frac{1}{2}}$. In these coordinates, the boundary of the elliptic vortex is represented by

$$\xi = \xi_0 = \tfrac{1}{2}\log((a+b)/(a-b)), \tag{7}$$

and the streamfunction outside the vortex is written as

$$\Psi_{out} = -\tfrac{1}{2}ab\xi - \tfrac{1}{4}ab\,e^{-2\xi}\cos 2\eta. \tag{8}$$

Since the basic flow is uniform in the vertical direction, we can introduce the normal-mode disturbances of the form

$$\psi_{in,\,out} = \Psi_{in,\,out} + \epsilon f(z)\,\hat{\psi}_{in,\,out}(\xi,\eta)\,e^{-i\omega t}, \quad (\epsilon \ll 1), \tag{9}$$

where $f(z)$ denotes the eigenfunction of a Sturm–Liouville problem associated with the differential operator L_z. With appropriate boundary conditions, $f(z)$ corresponds to the eigenvalue λ by

$$L_z f(z) = -\lambda^2 f(z). \tag{10}$$

The boundary of the vortex patch is assumed to deform as

$$\xi = \xi_0 + \epsilon F(\eta) f(z)\,e^{-i\omega t}. \tag{11}$$

Our objective is to determine the dispersion relation $\omega(\lambda)$. If it has a positive imaginary part, the vortex is known to be unstable to the mode corresponding to the value of λ.

We consider, solely, the perturbations that do not introduce additional potential vorticity. In other words, the disturbance streamfunctions (both inside and outside of the ellipse) obey the Helmholtz equation

$$(\nabla^2 + L_z)\,\hat{\psi}_{in,\,out} f(z) = 0,$$

or
$$(\nabla^2-\lambda^2)\hat{\psi}_{in,\,out}f(z)=0, \tag{12}$$

instead of
$$\left[\frac{\partial}{\partial t}+\frac{\partial \Psi_{in,\,out}}{\partial y}\frac{\partial}{\partial x}-\frac{\partial \Psi_{in,\,out}}{\partial x}\frac{\partial}{\partial y}\right](\nabla^2+\mathrm{L}_z)\hat{\psi}_{in,\,out}f(z)\,\mathrm{e}^{-\mathrm{i}\omega t}=0.$$

At $O(\epsilon)$, the kinematical boundary condition that the boundary of the vortex path continues to be the boundary is written, on $\xi=\xi_0$, as

$$\mathrm{i}\omega h^2F+\frac{\partial\hat{\psi}_{in}}{\partial\eta}-\Omega\frac{\partial}{\partial\eta}(h^2F)=0, \tag{13a}$$

$$\mathrm{i}\omega h^2F+\frac{\partial\hat{\psi}_{out}}{\partial\eta}-\Omega\frac{\partial}{\partial\eta}(h^2F)=0, \tag{13b}$$

where h^2 denotes the metric factor, i.e.
$$h^2=\tfrac{1}{2}c^2(\cosh 2\xi-\cos 2\eta).$$
The dynamical condition on $\xi=\xi_0$ is the continuity of tangential velocity, which is identical to the condition of pressure continuity:
$$\frac{\partial\hat{\psi}_{in}}{\partial\xi}-\frac{\partial\hat{\psi}_{out}}{\partial\xi}=h^2F\quad\text{at}\quad\xi=\xi_0. \tag{14}$$

We determine the eigenvalues numerically, based on a Galerkin method. In the elliptic-cylinder coordinates, the Helmholtz equation (12) has the form
$$\left[\frac{\partial^2}{\partial\xi^2}+\frac{\partial^2}{\partial\eta^2}-2q(\cosh 2\xi-\cos 2\eta)\right]\hat{\psi}_{in,\,out}=0 \tag{15}$$
with
$$q=\tfrac{1}{4}c^2\lambda^2,$$
which is separable. The solutions are expanded in terms of the mathieu functions as

$$\hat{\psi}^o_{in}=\sum_{m=1}^{\infty}[A^o_m\,\mathrm{ce}_{2m-1}(\eta,-q)\,\mathrm{Ce}_{2m-1}(\xi,-q)+B^o_m\,\mathrm{se}_{2m-1}(\eta,-q)\,\mathrm{Se}_{2m-1}(\xi,-q)], \tag{16a}$$

$$\hat{\psi}^o_{out}=\sum_{m=1}^{\infty}[C^o_m\,\mathrm{ce}_{2m-1}(\eta,-q)\,\mathrm{Ke}_{2m-1}(\xi,q)+D^o_m\,\mathrm{se}_{2m-1}(\eta,-q)\,\mathrm{Ko}_{2m-1}(\xi,q)], \tag{16b}$$

$$\hat{\psi}^e_{in}=\sum_{m=1}^{\infty}[A^e_m\,\mathrm{ce}_{2m-2}(\eta,-q)\,\mathrm{Ce}_{2m-2}(\xi,-q)+B^e_m\,\mathrm{se}_{2m}(\eta,-q)\,\mathrm{Se}_{2m}(\xi,-q)], \tag{17a}$$

$$\hat{\psi}^e_{out}=\sum_{m=1}^{\infty}[C^e_m\,\mathrm{ce}_{2m-2}(\eta,-q)\,\mathrm{Ke}_{2m-2}(\xi,q)+D^e_m\,\mathrm{se}_{2m}(\eta,-q)\,\mathrm{Ko}_{2m}(\xi,q)], \tag{17b}$$

where the solution with the superscript o/e is 2π-periodic (odd)/π-periodic (even) in the variable η. They are decoupled because of the Z_2-symmetry of the basic flow field, i.e. because Kirchhoff's elliptic vortex is π-periodic in η. The functions ce and se denote the Mathieu functions and Ce, Se, Ke and Ko are the modified Mathieu functions (see e.g. Abramowitz & Stegun 1972). Robinson & Saffman (1984) used similar expansions in an analysis of the three-dimensional instability of an elliptical vortex in a straining field. The characteristic values and the functional values of the Mathieu functions (and the modified Mathieu functions Ce and Se) are computed using appropriate routines and their modifications (e.g. Clemm 1969; Blanch 1966; Sale 1970). The functional values of the modified Mathieu functions Ke and Ko are determined by integrating the governing equation numerically (see, for details, Robinson & Saffman 1984).

As the procedure of the formulation of the eigenvalue problem is well known, we will outline only the case of the odd modes. We notice from the boundary conditions (13*a*) and (13*b*) that $\hat{\psi}_{in}(\xi_0) = \hat{\psi}_{out}(\xi_0)$. Then we introduce the new coefficients E and F instead of A, B, C and D, as

$$A_m^o = \frac{E_m^o}{\mathrm{Ce}_{2m-1}(\xi_0, -q)}, \quad B_m^o = \frac{F_m^o}{\mathrm{Se}_{2m-1}(\xi_0, -q)}, \quad C_m^o = \frac{E_m^o}{\mathrm{Ke}_{2m-1}(\xi_0, q)},$$

$$D_m^o = \frac{F_m^o}{\mathrm{Ko}_{2m-1}(\xi_0, q)}. \tag{18}$$

Eliminating h^2F from (13*a*) using (14), we have

$$\begin{aligned}
&\mathrm{i}\omega \sum_{m=1}^{N} \left[E_m^o \,\mathrm{ce}_{2m-1}(\eta, -q) \left\{ \frac{\mathrm{Ce}'_{2m-1}(\xi_0, -q)}{\mathrm{Ce}_{2m-1}(\xi_0, -q)} - \frac{\mathrm{Ke}'_{2m-1}(\xi_0, q)}{\mathrm{Ke}_{2m-1}(\xi_0, q)} \right\} \right. \\
&\qquad \left. + F_m^o \,\mathrm{se}_{2m-1}(\eta, -q) \left\{ \frac{\mathrm{Se}'_{2m-1}(\xi_0, -q)}{\mathrm{Se}_{2m-1}(\xi_0, -q)} - \frac{\mathrm{Ko}'_{2m-1}(\xi_0, q)}{\mathrm{Ko}_{2m-1}(\xi_0, q)} \right\} \right] \\
&\qquad + \sum_{m=1}^{N} \left[E_m^o \,\mathrm{ce}'_{2m-1}(\eta, -q) + F_m^o \,\mathrm{se}'_{2m-1}(\eta, -q) \right] \\
&-\Omega \sum_{m=1}^{N} \left[E_m^o \,\mathrm{ce}'_{2m-1}(\eta, -q) \left\{ \frac{\mathrm{Ce}'_{2m-1}(\xi, -q)}{\mathrm{Ce}_{2m-1}(\xi_0, -q)} - \frac{\mathrm{Ke}'_{2m-1}(\xi_0, q)}{\mathrm{Ke}_{2m-1}(\xi, q)} \right\} \right. \\
&\qquad \left. + F_m^o \,\mathrm{se}'_{2m-1}(\eta, -q) \left\{ \frac{\mathrm{Se}'_{2m-1}(\xi_0, -q)}{\mathrm{Se}_{2m-1}(\xi_0, -q)} - \frac{\mathrm{Ko}'_{2m-1}(\xi_0, q)}{\mathrm{Ko}_{2m-1}(\xi_0, q)} \right\} \right] = 0,
\end{aligned} \tag{19}$$

where primes denote differentiation with respect to ξ_0 or η. Truncating the expansions at a finite order N, making the products of (19) with $\mathrm{ce}_{2l-1}(\eta, -q)$ and $\mathrm{se}_{2l-1}(\eta, -q)$ ($1 \leqslant l \leqslant N$: Galerkin method), and integrating from 0 to 2π, we obtain the following matrix-type relation:

$$(\mathrm{i}\omega \boldsymbol{A} - \boldsymbol{B}) \begin{pmatrix} E_1^o \\ \vdots \\ E_N^o \\ F_1^o \\ \vdots \\ F_N^o \end{pmatrix} = 0. \tag{20}$$

Here the matrix $\boldsymbol{A}$ is a $2N \times 2N$ diagonal matrix. The eigenvalues ω and the eigenvectors $(E_j^o, F_j^o)^t$ of the matrix $-\mathrm{i}\boldsymbol{A}^{-1}\boldsymbol{B}$ ($2N \times 2N$) are calculated numerically using the QR method. The truncation order N, which is typically 20, is increased up to 40 when it is necessary to achieve accuracy of four significant figures. The eigenvalues form either real pairs or pure imaginary pairs of opposite sign. In the latter pairs, one with positive imaginary part corresponds to an unstable mode. Using the eigenvectors $(E_j^o, F_j^o)^t$ thus obtained, the disturbance streamfunction $\hat{\psi}$ can be calculated by (16*a*, *b*) and (18). The stability characteristics are illustrated in the next section.

3. Results

Since the odd (2π-periodic) and even (π-periodic) modes are decoupled completely, we will describe the results for the odd modes in §3.1 and those for the even modes in §3.2, separately.

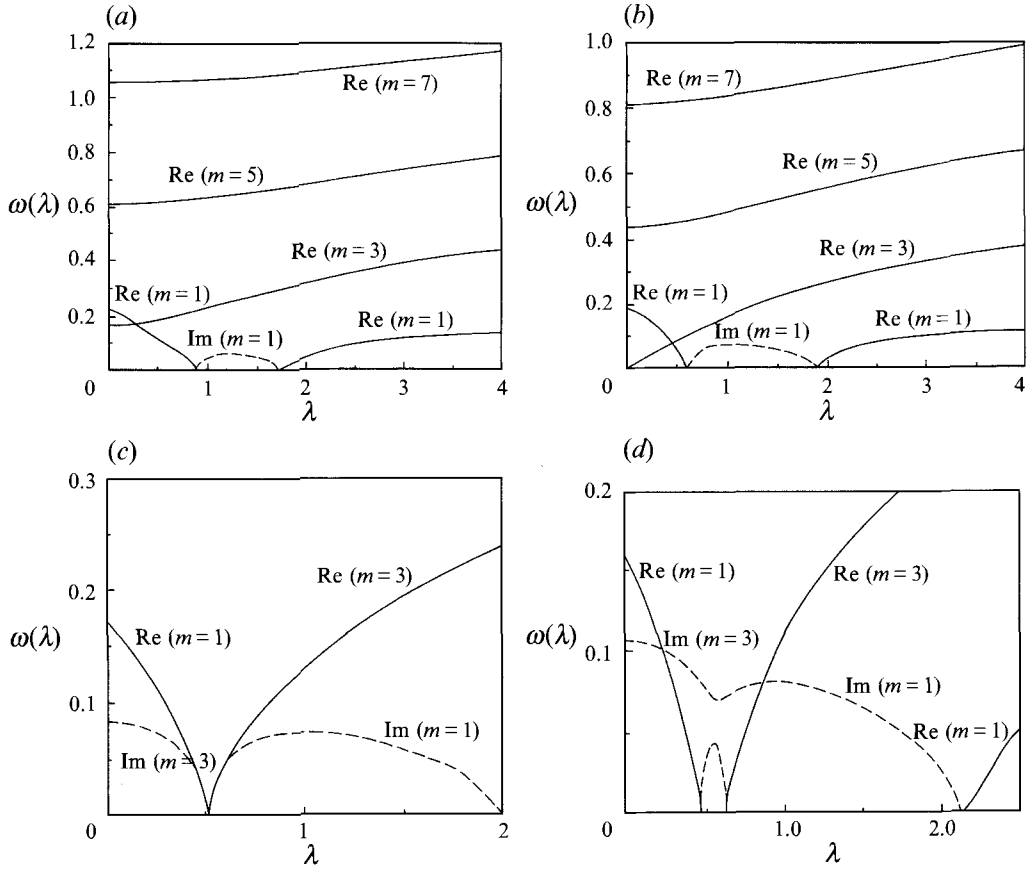

FIGURE 1. Dispersion relation $\omega(\lambda)$ of the odd modes for ellipses of (*a*) $a/b = 2$, (*b*) $a/b = 3$, (*c*) $a/b = 3.5$ and (*d*) $a/b = 4$. The horizontal axis is the vertical wavenumber λ and the vertical axis is the calculated $\omega(\lambda)$. Solid lines trace real (stable) $\omega(\lambda)$ and broken lines represent pure imaginary (unstable) $\omega(\lambda)$.

3.1. 2π-*periodic* (*odd*) *modes*

We show in figure 1 (*a–d*) the calculated dispersion relation for the cases $a/b = 2$, 3, 3.5 and 4, respectively. The horizontal axis is the vertical wavenumber λ (the eigenvalue of L_z) and the vertical axis is the real or imaginary part of ω. Solid lines trace real (stable) ω and broken lines represent pure imaginary (unstable) ω. In the limit of $\lambda \to 0$, our results agree with Love's barotropic result for ω, given by

$$\omega^2 = \frac{1}{4}\left[\left(\frac{2mab}{(a+b)^2} - 1\right)^2 - \left(\frac{a-b}{a+b}\right)^{2m}\right]. \tag{21}$$

Here, the integer m is the azimuthal wavenumber. For $a/b < 3$, all the barotropic modes ($\lambda = 0$) are stable, as we can see in Figure 1 (*a*, *b*). When a/b is larger than 3, the $m = 3$ mode grows exponentially (figure 1 *c*, *d*), whereas other modes remain stable.

It is remarkable that there is a λ-range ($0.88 < \lambda < 1.70$) where the bending mode ($m = 1$) grows even for the barotropically stable ellipse of $a/b = 2$ (figure 1 *a*). This unstable range is away from the ω-axis, indicating that the instability is a short-wave instability. We depict the perturbed vortex boundary and the disturbance

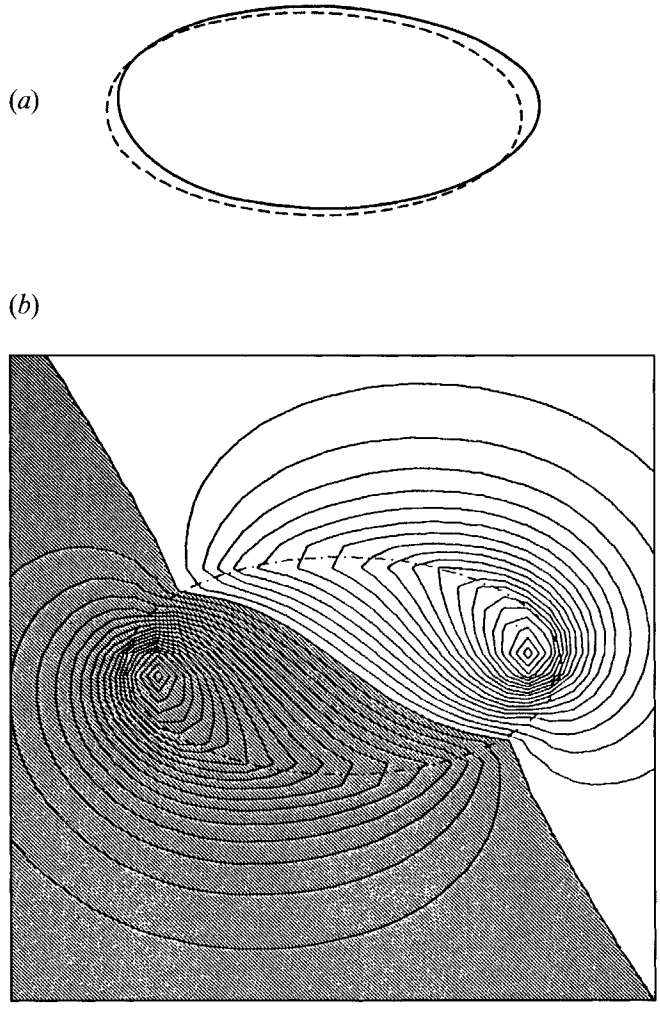

FIGURE 2. (*a*) Perturbed vortex boundary of the ellipse of $a/b = 2$. The disturbance has vertical wavenumber $\lambda = 1.25$ and the characteristic azimuthal wavenumber $m = 1$. (*b*) Disturbance streamlines. The hatched region corresponds to negative values of the streamfunction.

streamfunction for $\lambda = 1.25$ in figures 2(*a*) and 2(*b*), respectively. We can see clearly that the instability mode has an azimuthal wavenumber 1 and a phase shift of about $\frac{1}{4}\pi$ (to the major semi-axis). The shape of the deformed vortex patch resembles contours of constant height (Meacham 1992, figure 17) of an unstable (M2I mode) ellipsoid with semi-axes of $\sqrt{2}$, $1/\sqrt{2}$ and 1.

The case of $a/b = 3$ (figure 1*b*) is marginal. The $m = 3$ mode is just destabilized at the long-wave limit ($\lambda \to 0$). The short-wave instability is also enhanced as a/b becomes larger. The instability ranges of the short-wave ($m = 1$) mode and the long-wave ($m = 3$) mode merge when a/b is increased above 3.5 (figure 1*c*, *d*). Two instability modes are observed in figure 1(*d*), where the major (stronger) mode has a wider instability λ-range ($0 < \lambda < 2.10$) and the minor has a narrower λ-range ($0.45 < \lambda < 0.63$). It is not appropriate that we call the major one the '$m = 3$ mode' and the minor one the '$m = 1$ mode', since, as we will also see in figures 3–5, the characteristic azimuthal wavenumber of the major mode changes from 3 to 1 as λ increases. On the other hand, the azimuthal wavenumber of the minor mode changes from 1 to 3 as λ

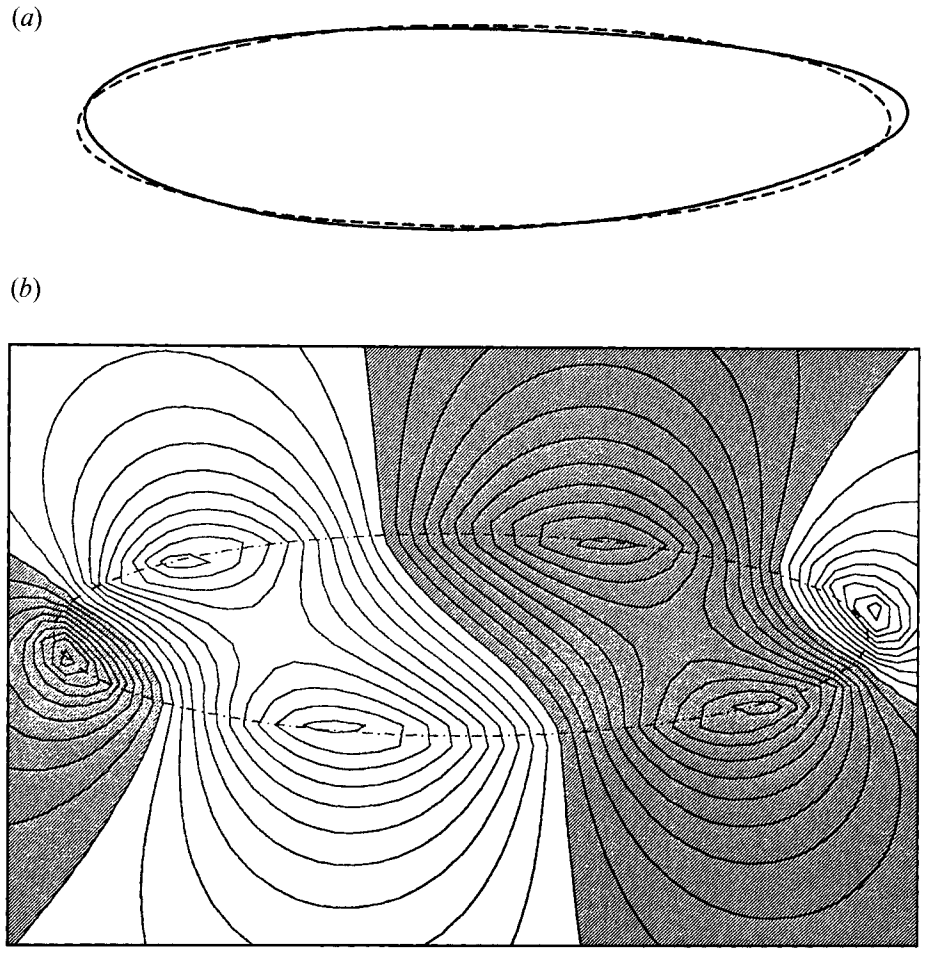

FIGURE 3. (*a*) Perturbed vortex boundary of the ellipse of $a/b = 4$. The disturbance has the vertical wavenumber $\lambda = 0.1$ and the characteristic azimuthal wavenumber $m = 3$. (*b*) Disturbance streamlines.

increases. Figures 3–5 show the perturbed vortex boundary (parts *a*) and the disturbance streamfunction (parts *b*) for $\lambda = 0.1$, 0.55 and 1.0, respectively. We can observe the change of the characteristic azimuthal wavenumber. The vortex boundary in figure 3(*a*) ($m = 3$ mode) has a slight resemblance to that of Meacham's M3I unstable mode (Meacham 1992, figure 18), although the ratio a/b is not the same. The reason why such mode coupling occurs is that the basic flow field is not axisymmetric but has only Z_2-symmetry. It is also found in quantum-mechanical band calculations that two curves representing two energy levels do not cross each other but split.

As a/b is increased further, higher mode will be destabilized successively. An instability mode that continues to a barotropic mode of azimuthal wavenumber larger than or equal to 3, is *essentially* a long-wave instability. The bending mode ($m = 1$) for $a/b < 3$, in contrast, is *essentially* a short-wave instability. Figure 6 shows contours of constant growth rate in the (λ, a/b)-plane, where the horizontal axis is the vertical wavenumber λ, the vertical axis is the aspect ratio a/b and the contour interval is 0.01. It is remarkable that Kirchhoff's elliptic vortex is unstable to the bending mode ($m = 1$) irrespective of a/b for a certain range of λ and that the unstable region touches

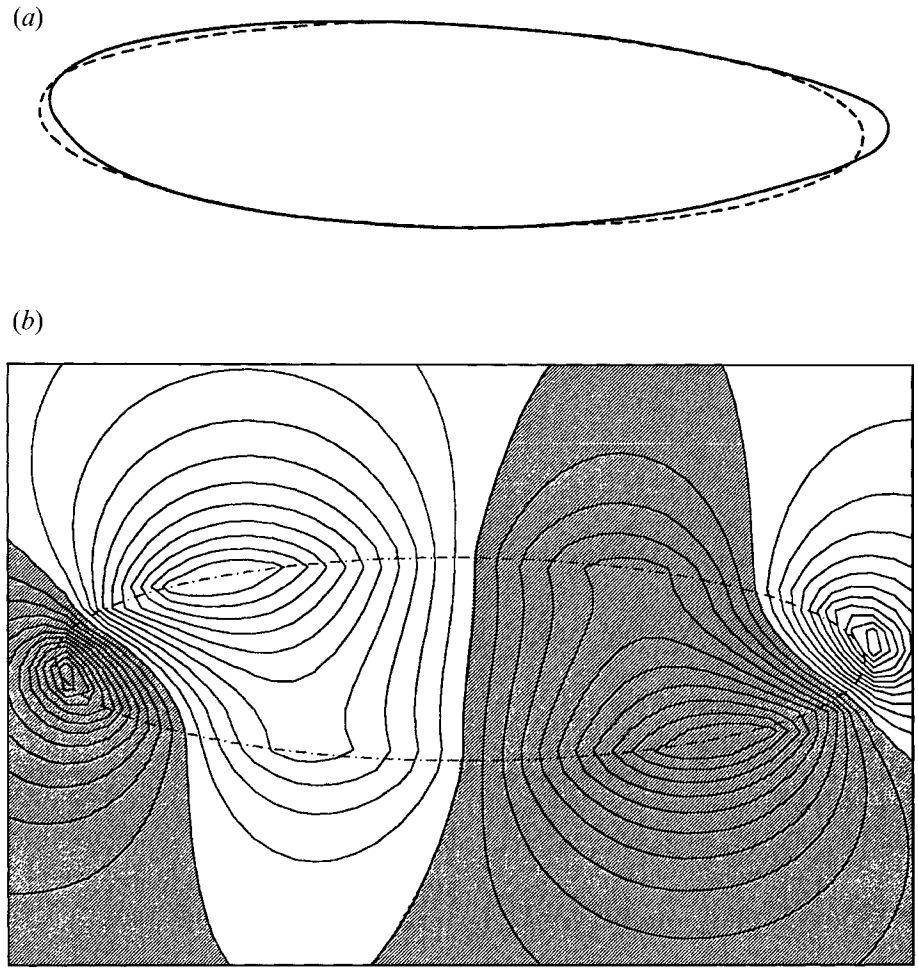

FIGURE 4. As figure 3 but for $\lambda = 0.55$ and a vague characteristic azimuthal wavenumber.

the λ-axis at $\lambda = \lambda_c = 1.7046$. Close examination shows that the growth rate of the bending mode is proportional to $a/b - 1$, when it is close to 0. Using figure 6, we can judge whether an ellipse of a given aspect ratio a/b is stable or unstable, if the spectrum $\{\lambda_n\}$ of the Sturm–Liouville problem (10) is known. We will consider the physical mechanism of the instability in §4, where the meaning of the critical wavenumber λ_c is explained. The origin of the instability is traced back to the resonant interaction between the bending baroclinic wave ($m = 1$) and the $m = 2$ barotropic wave.

3.2. π-*periodic* (*even*) *modes*

Regarding even modes, Love's formula (21) tells that any barotropic mode is stable until a/b exceeds 4.612, where the $m = 4$ mode destabilizes first. Figure 7, on the other hand, shows that there is an unstable λ-range ($0 < \lambda < 0.85$) even for a barotropically stable ellipse of $a/b = 2$. It is an $m = 2$ baroclinic instability, which can also be seen from the shape of the deformed vortex patch and the perturbation streamfunction in figures 8(*a*) and 8(*b*) ($\lambda = 0.5$). Although the growth rate vanishes in the limit of $\lambda \to 0$, the instability region is attached to the a/b-axis and the instability is thought of as a long-wave instability. The physical mechanism of this instability seems to be

(*a*)

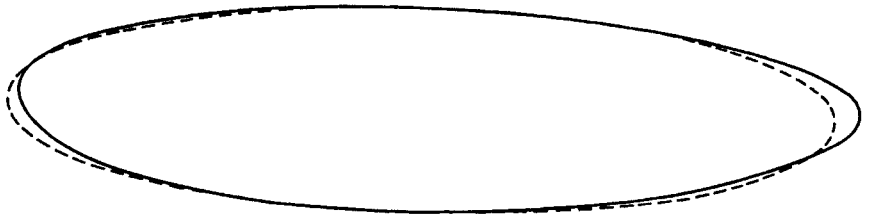

(*b*)

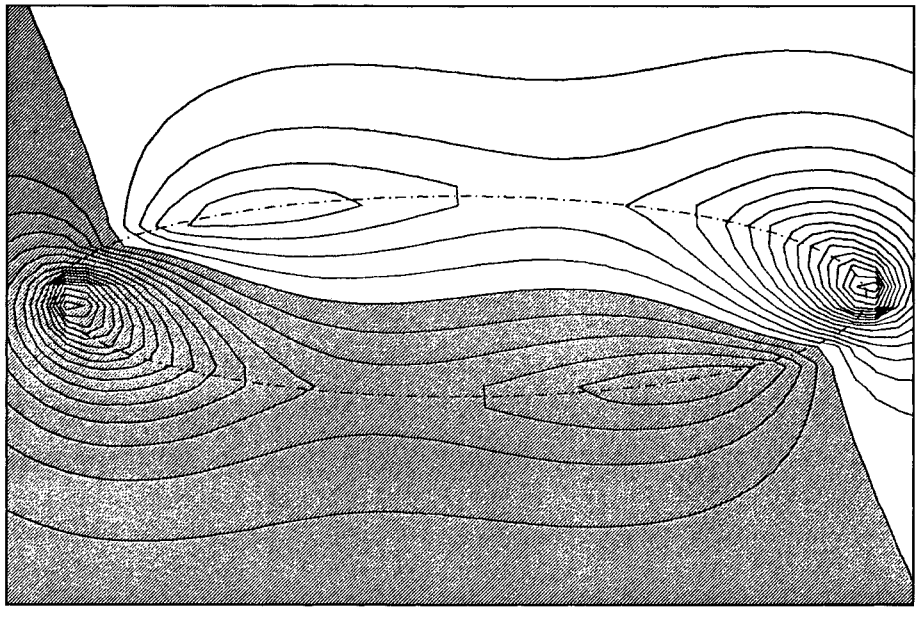

FIGURE 5. As figure 3 but for $\lambda = 1.0$ and the characteristic azimuthal wavenumber $m = 1$.

related to a sideband instability (Benjamin–Feir instability) of finite-amplitude barotropic waves. We will discuss this in more detail in the following section.

Figure 9 depicts contours of constant growth rate in the $(\lambda, a/b)$-plane. Only the $m = 2$ mode appears in the parameter region described in this figure ($a/b < 4$). Any ellipse is unstable to the $m = 2$ baroclinic mode irrespective of the value of a/b. The growth rate increases and the unstable λ-range becomes wider as the ratio a/b increases. Close examination shows that the growth rate decays like $(a/b-1)^2$ in the limit $a/b \to 1$. From figure 9, we can judge whether an ellipse is stable or unstable to π-periodic disturbances, if information about the spectrum $\{\lambda_n\}$ of the Strum–Loiuville problem (10) is provided.

We will comment briefly on the spectrum $\{\lambda_n\}$ of the Sturm–Liouville problem (10) before closing this section. The differential operator L_z takes a simple form when the fluid has a constant Brunt–Väisälä frequency N_s. In the case of the oceanic synoptic scale, (2*b*) becomes

$$\mathrm{L}_z = \frac{1}{S}\frac{\partial^2}{\partial z^2} = \left(\frac{L}{L_D}\right)^2 \frac{\partial^2}{\partial z^2}, \tag{22}$$

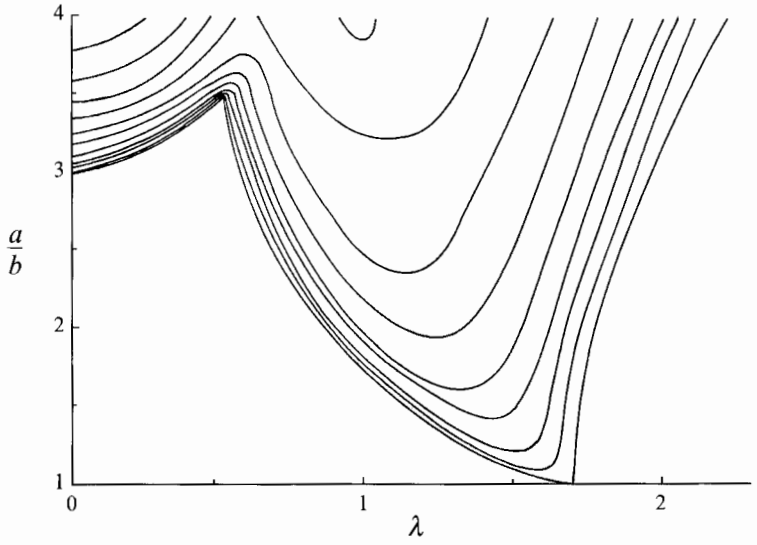

FIGURE 6. Contours of constant growth rate of the odd instability modes. The horizontal axis is the vertical wavenumber λ and the vertical axis is a/b. The contour interval is 0.01. The instability region touches the λ-axis at $\lambda_c = 1.7046$.

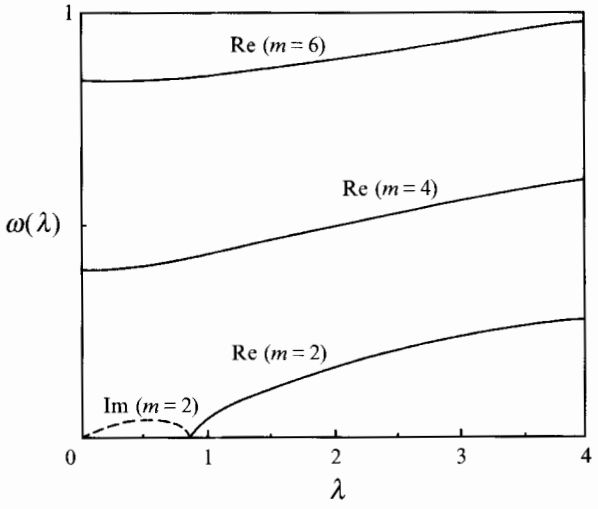

FIGURE 7. Dispersion relation $\omega(\lambda)$ of the even modes for the ellipse of $a/b = 2$. The horizontal axis is the vertical wavenumber λ and the vertical axis is the calculated $\omega(\lambda)$. Solid lines trace real (stable) $\omega(\lambda)$ and broken lines represent pure imaginary (unstable) $\omega(\lambda)$.

where $L_D = N_s D/f$ is the internal Rossby radius of deformation, and L and D denote the horizontal and vertical lengthscales, respectively (see Pedlosky 1979, §6). Imposing the condition of no tangential stress at the upper ($z = 1$) and lower ($z = 0$) boundaries, implies that

$$\frac{\partial \psi}{\partial z} = 0, \quad \text{at} \quad z = 0, 1 \tag{23}$$

and we obtain the spectrum $\{\lambda_n = n\pi L/L_D$: n is an integer$\}$. Thus, an ellipse whose

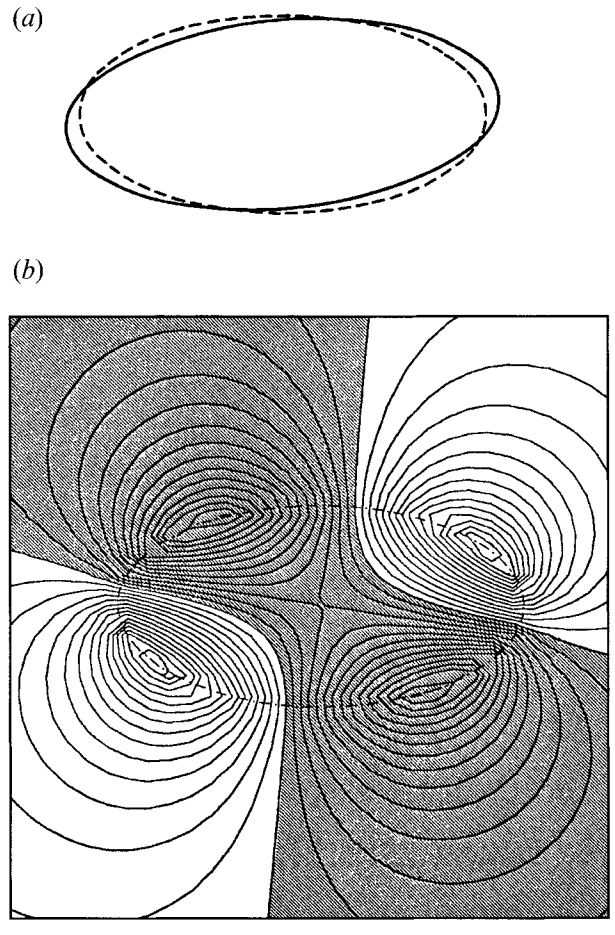

FIGURE 8. (*a*) Perturbed vortex boundary of the ellipse of $a/b = 2$ The disturbance has the vertical wavenumber $\lambda = 0.5$ and the characteristic azimuthal wavenumber $m = 2$. (*b*) Disturbance streamlines. The hatched region corresponds to negative values of the streamfunction.

horizontal scale L is small compared to L_D (a typical value of L_D for the ocean is $O(100\text{ km})$) may become unstable for the baroclinic modes that satisfy $\lambda_n < O(1)$, as we expect from figures 6 and 9.

4. Physical mechanisms

The aim of this section is twofold. First, we give a clear physical interpretation of two baroclinic instability modes, i.e. the $m = 1$ (bending wave) and the $m = 2$ (elliptical deformation) modes. Second, an apparent contradiction between our result, which predicts the occurrence of order-$\epsilon'(= a/b - 1)$ instability in the limit of $\epsilon' \to 0$, and Dritschel's stability criterion which states that a circular vortex patch is nonlinearly stable, is resolved.

Let us consider the dispersion relation of an inertial wave on Rankine's combined vortex (in the circular-vortex limit of $\epsilon' \to 0$). The streamfunction of the basic flow field is given in cylindrical coordinates (r, θ, z), as

$$\Psi_{in} = -\tfrac{1}{4}r^2 \quad \text{for} \quad r < 1, \qquad \Psi_{out} = -\tfrac{1}{4} - \tfrac{1}{2}\log r \quad \text{for} \quad r \geqslant 1. \qquad (24a, b)$$

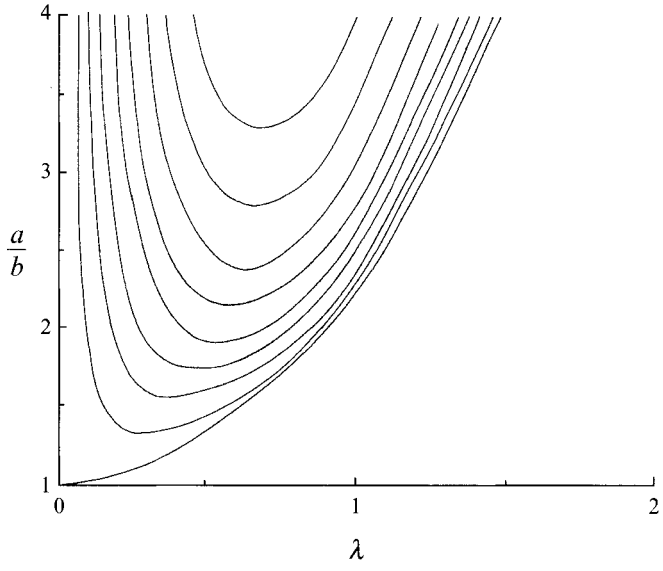

FIGURE 9. Contours of constant growth rate of the even instability modes. The horizontal axis is the vertical wavenumber λ and the vertical axis is a/b. The contour interval is 0.01. The instability region touches the λ-axis at the origin.

Since the disturbance streamfunction satisfies the Helmholtz equation, we can introduce the following normal modes:

$$\psi'_{in} = aI_m(\lambda r)f(z)\,\mathrm{e}^{\mathrm{i}(m\theta-\omega t)} \quad \text{for} \quad r<1, \tag{25a}$$

$$\psi'_{out} = bK_m(\lambda r)f(z)\,\mathrm{e}^{\mathrm{i}(m\theta-\omega t)} \quad \text{for} \quad r>1, \tag{25b}$$

$$\delta r = cf(z)\,\mathrm{e}^{\mathrm{i}(m\theta-\omega t)}. \tag{26}$$

Here, I_m and K_m denote modified Bessel functions of the mth order. The boundary conditions corresponding to (13a, b) and (14) are imposed at $r=1$:

$$\left[\frac{\partial}{\partial t}+\frac{\partial \Psi_{in,\,out}}{\partial y}\frac{\partial}{\partial x}-\frac{\partial \Psi_{in,\,out}}{\partial x}\frac{\partial}{\partial y}\right](r-1-\delta r)=0, \tag{27a, b}$$

$$\frac{\partial}{\partial r}\psi'_{in}=\frac{\partial}{\partial r}\psi'_{out}. \tag{28}$$

These three equations form a set of linear, homogeneous equations in a, b and c and are mutually consistent if the determinant of their coefficients is zero. This leads to the dispersion relation

$$\omega(m,\lambda)=m[\tfrac{1}{2}-I_m(\lambda)\,K_m(\lambda)]. \tag{29}$$

It should be noted that (29) is the dispersion relation in a stationary frame, which differs by $\Omega_{a=b}=\frac{1}{4}$ from (21) (putting $a=b$), which is the dispersion relation in a rotating frame. Figure 10 shows the dispersion relation of the bending mode $m=1$, where the horizontal and vertical axes are λ and ω, respectively. We notice, at once, the meaning of the critical wavenumber $\lambda_c=1.7046$ that appeared in the previous section (figure 6). It corresponds to $\omega_c=0.25$, which is the rotation rate of the $m=2$ barotropic wave, i.e. $\frac{1}{2}\omega(2,0)$. The bending baroclinic wave of $\lambda_c=1.7046$ rotates in phase with the elliptic deformation wave and the resonant interaction between these two waves seems to cause the instability. Dritschel's nonlinear-stability bounds,

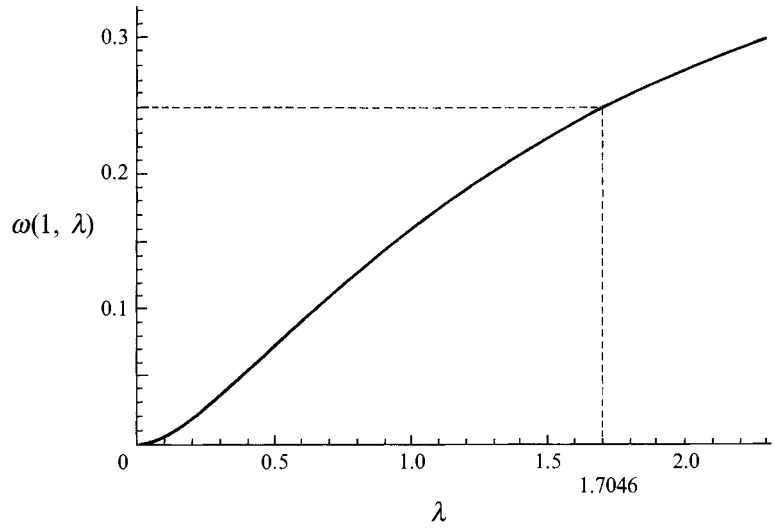

FIGURE 10. Dispersion relation of the bending wave ($m = 1$) on Rankine's combined vortex. The horizontal axis is the vertical wavenumber λ and the vertical axis is $\omega(1, \lambda)$. Note that $\omega(1, \lambda_c) = 0.25$.

however, strongly constrain the time-evolution of a circular vortex patch. Weakly-nonlinear interactions between two waves should be considered in more detail, before drawing a conclusion.

Let us study the resonant interaction between the bending baroclinic wave of $\lambda = \lambda_c$ and the $m = 2$ barotropic wave, following the procedure of multiscale expansions (e.g. Craik 1985). We introduce disturbances, up to second order, of the form

$$\psi'_{in} = \epsilon A(\tau)\frac{I_1(\lambda_c r)}{4I_1(\lambda_c)}f_c(z)\,\mathrm{e}^{\mathrm{i}(\theta - t/4)} + \tfrac{1}{4}\epsilon B(\tau)\,r^2\,\mathrm{e}^{2\mathrm{i}(\theta - t/4)} + \text{c.c.} + \epsilon^2\psi'^{(2)}_{in}, \tag{30a}$$

$$\psi'_{out} = \epsilon A(\tau)\frac{K_1(\lambda_c r)}{4K_1(\lambda_c)}f_c(z)\,\mathrm{e}^{\mathrm{i}(\theta - t/4)} + \frac{\epsilon}{4r^2}B(\tau)\,\mathrm{e}^{2\mathrm{i}(\theta - t/4)} + \text{c.c.} + \epsilon^2\psi'^{(2)}_{out}, \tag{30b}$$

$$\delta r = \epsilon A(\tau)f_c(z)\,\mathrm{e}^{\mathrm{i}(\theta - t/4)} + \epsilon B(\tau)\,\mathrm{e}^{2\mathrm{i}(\theta/t/4)} + \text{c.c.} + \epsilon^2\delta r^{(2)}. \tag{31}$$

Here, $\tau = \epsilon t$ denotes a slow time variable and $f_c(z)$ is the eigenfunction corresponding to λ_c. From (31), we notice that the semi-major and semi-minor axes of the ellipse are $a = 1 + 2\epsilon B$ and $b = 1 - 2\epsilon B$, respectively, so the ratio a/b is given by $1 + 4\epsilon B (= 1 + \epsilon')$. Substituting (30$a$, b) and (31) into the nonlinear boundary conditions imposed at $r = 1 + \delta r$ (whose linear forms are (27a, b) and (28)), we get inhomogeneous equations for the second-order quantities. The solvability conditions yield the time evolution of A and B, as (see Appendix for details)

$$\mathrm{i}\frac{\mathrm{d}A}{\mathrm{d}\tau} = \alpha\bar{A}B, \qquad \mathrm{i}\frac{\mathrm{d}B}{\mathrm{d}\tau} = \beta A^2, \tag{32a, b}$$

where

$$\alpha = \frac{1}{2}\left(2 - \frac{\lambda_c I_0(\lambda_c)}{I_1(l_c)}\right) = 0.3259, \tag{33}$$

$$\beta = \alpha\int_{z_b}^{z_t}\rho_s f_c^2(z)\,\mathrm{d}z \Big/ \int_{z_b}^{z_t}\rho_s\,\mathrm{d}z. \tag{34}$$

The integral factor (34) measures the magnitude of the coupling of $f_c^2(z)$ with the barotropic mode. Here, the differential operator L_z is assumed to have the form (2*a*) (i.e. for atmospheric synoptic-scale phenomena)

$$\mathrm{L}_z = \frac{1}{\rho_s}\frac{\partial}{\partial z}\left(\frac{\rho_s}{S}\frac{\partial}{\partial z}\right).$$

We have chosen this L_z because it is convenient in a comparison with Dritschel's result. We can take the 'standard' density ρ_s to be unity for oceanic synoptic-scale phenomena (see (2*b*) and (22)).

We now consider (32*a*, *b*). If we are interested in the linear stability of a slightly elongated ellipse $a/b = 1+\epsilon$, we may put $B = \frac{1}{4}$ (then we have $\epsilon' = \epsilon$) and follow only the time evolution of (32*a*). We find a solution that grows exponentially:

$$A = |A(0)|\,\mathrm{e}^{(\alpha\tau - \mathrm{i}\pi)/4}. \tag{36}$$

This explains the order-$\epsilon'(=\epsilon)$ instability found in the previous section. In fact, the amplification factor $\frac{1}{4}\alpha = 0.0815$ is close to the numerically evaluated value 0.081 and the phase shift of $\pi/4$ can be evaluated in figure 2(*a*), although $a/b-1 = 1$ is not so small there. Thus, the resonant interaction between these two waves does play a key role in the baroclinic bending wave instability.

At first sight, it seems that the presence of such an instability and Dritschel's strong stability theorem contradict each other. However, it is now clear that the linear instability of an infinitesimally deformed (elliptic) vortex patch does not imply weakly nonlinear instability of a circular vortex patch. It is not difficult to see, from (32*a*, *b*), that

$$\frac{\mathrm{d}}{\mathrm{d}\tau}\left(A\bar{A}\int_{z_b}^{z_t}\rho_s f_c^2\,\mathrm{d}z + B\bar{B}\int_{z_b}^{z_t}\rho_s\,\mathrm{d}z\right) = 0. \tag{37}$$

This describes the conservation of a second-order quantity, and it is an approximate formula (up to second order) for the mean normal displacement of a vortex boundary from its undisturbed circular position, found by Dritschel (1988*a*, equation (9)). The bending instability will saturate unless the basic elliptical deformation is maintained somehow. Any ellipse, more generally, can be thought of as an irrotationally deformed form of a circle (of radius $(ab)^{\frac{1}{2}}$) and its nonlinear evolution is strongly constrained by Dritschel's stability bounds. It would be interesting to investigate the later stage of nonlinear baroclinic development of a perturbed Kirchhoff's elliptic vortex.

Similarly, we can get a clear physical interpretation of the even instability mode, if we consider the weakly nonlinear evolution of the $m = 2$ barotropic wave. Instead of (30*a*, *b*) and (31) we introduce disturbances of the form:

$$\psi'_{in} = \tfrac{1}{4}\epsilon C(\tau,\xi)\,r^2\,\mathrm{e}^{2\mathrm{i}(\theta - t/4)} + \text{c.c.} + \epsilon^2\psi'^{(2)}_{in} + \epsilon^3\psi'^{(3)}_{in}, \tag{38a}$$

$$\psi'_{out} = \frac{\epsilon}{4r^2}C(\tau,\xi)\,\mathrm{e}^{2\mathrm{i}(\theta - t/4)} + \text{c.c.} + \epsilon^2\psi'^{(2)}_{out} + \epsilon^3\psi'^{(3)}_{out}, \tag{38b}$$

$$\delta r = \epsilon C(\tau,\xi)\,\mathrm{e}^{2\mathrm{i}(\theta - t/4)} + \text{c.c.} + \epsilon^2\delta r^{(2)} + \epsilon^3\delta r^{(3)}, \tag{39}$$

where τ and ξ denote slow variables $\epsilon^2 t$ and $\epsilon(z - C_g t)$, respectively, with C_g the group velocity $(\partial\omega/\partial\lambda)_{\lambda=0}$. Substituting (38*a*, *b*) and (39) into the boundary conditions (27*a*, *b*) and (28), we obtain inhomogeneous equations for the second- and third-order quantities. The solvability condition of the second-order equation gives $C_g = 0$, whereas that of the third-order equation yields a nonlinear Schrödinger equation:

$$\mathrm{i}\frac{\partial C}{\partial\tau} + \mu\frac{\partial^2 c}{\partial\xi^2} + \nu|C|^2 C = 0,$$

with $$\mu = \frac{1}{2}\left(\frac{\partial^2 \omega}{\partial \lambda^2}\right)_{\lambda=0} = \frac{1}{12}$$

and $\nu = 2$. Dritschel (1988*b*) presents an analysis of weakly nonlinear evolution of a barotropic wave with general azimuthal wavenumber. The finite-amplitude solution $C = C_0 e^{2i C_0^2 \tau}$ (weakly nonlinear Kirchhoff's ellipse) becomes unstable to a long-wave disturbance $0 < \lambda < 4\sqrt{3}\epsilon C_0$ (Benjamin–Feir instability; see Benjamin & Feir 1967). If we take, again, $C_0 = \frac{1}{4}$ for an ellipse of $a/b = 1+\epsilon$, then an unstable λ-range of width $\sqrt{3}\epsilon$ is expected in the limit of $\epsilon \to 0$ with a maximum growth rate $\frac{1}{2}\epsilon^2$ at $\lambda = \sqrt{6}/2\epsilon$. This is the physical interpretation of the $m = 2$ long-wave instability. Since a nonlinear Schrödinger equation is completely integrable and has an infinite number of conserved quantities, our findings are again consistent with Dritchel's stability criterion.

5. Summary and discussion

We have investigated the linear baroclinic instability of Kirchhoff's elliptic vortex, under the quasi-geostrophic, *f*-plane approximation. Any ellipse, irrespective of the ratio a/b(= semi-major axis/semi-minor axis), is shown to be unstable to the $m = 1$ bending mode and the $m = 2$ elliptical deformation mode. We have made an attempt to find a physical interpretation of these instability modes in the limit of small ellipticity. The former instability occurs as the result of resonant interaction between the baroclinic bending wave and the barotropic elliptical deformation wave. The latter instability can be thought of as a sideband (Benjamin–Feir) instability of a finite-amplitude $m = 2$ barotropic wave.

Recent numerical calculations of geostrophic turbulence (e.g. McWilliams 1989, 1990) demonstrate the emergence and growth to dominance of isolated, coherent vortices in the later stage of their time evolution. It would be of interest to consider the roles of the baroclinic instabilities found in this paper, for example the absence of highly elongated vortices. Such considerations, however, should not neglect the influence of the strain field locally imposed on a vortex. A strain field seems to enhance baroclinic instabilities, since it plays an essential role in the three-dimensional destabilization of a coherent vortex in a homogeneous fluid (e.g. Widnall, Bliss & Tsai 1974; Moore & Saffman 1975; Tsai & Widnall 1976). Although details are left for future work, we have already found that the bending instability is enhanced in magnitude but that its instability λ-range moves to the left (long-wave direction) for the stationary strained ellipse considered by Robinson & Saffman (1984) (see also Moore & Saffman 1971).

Kida (1981) investigated the two-dimensional motion of an elliptical vortex patch in a uniform background strain and vorticity field. He showed that the elliptical shape is retained whereas the axis ratio a/b changes with time. Dritschel (1990) studied the barotropic instability of the periodic Kida solutions and found that a significant portion of the periodic solutions is linearly unstable. Our next problem is to investigate the baroclinic instability of the Kida-type vortex under the quasi-geostrophic approximation.

We are grateful to Dr Y. Fukumoto for valuable comments and discussions during this study. We owe much to K. Hirahara in preparing the figures.

Appendix. The derivation of (32*a*, *b*) with (33) and (34)

General discussion on resonant wave interactions is presented in Craik (1985). First, we rewrite the three boundary conditions imposed at $r = 1+\delta r$ as

$$\Psi_{in}+\psi'_{in} = \Psi_{out}+\psi'_{out}, \tag{A 1}$$

$$\frac{\partial}{\partial r}(\Psi_{in}+\psi'_{in}) = \frac{\partial}{\partial r}(\Psi_{out}+\psi'_{out}), \tag{A 2}$$

$$\left[\frac{\partial}{\partial t}+\frac{1}{r}\frac{\partial}{\partial\theta}(\Psi_{in}+\psi'_{in})\frac{\partial}{\partial r}-\frac{1}{r}\frac{\partial}{\partial r}(\Psi_{in}+\psi'_{in})\frac{\partial}{\partial\theta}\right][r-1-\delta r] = 0 \tag{A 3}$$

Substitution of (25*a*, *b*) and (26) into (A 1)–(A 3) yields the linear relations:

$$L_m\begin{pmatrix}a\\b\\c\end{pmatrix} = \begin{pmatrix} I_m(\lambda) & -K_m(\lambda) & 0\\ \lambda I'_m(\lambda) & -\lambda K'_m(\lambda) & -1\\ mI_m(\lambda) & 0 & \omega-\frac{1}{2}m\end{pmatrix}\begin{pmatrix}a\\b\\c\end{pmatrix} = 0. \tag{A 4}$$

We obtain the dispersion relation (29) by putting the determinant of L_m to be zero.

Let us consider the resonant interaction. Substituting (30*a*, *b*) and (31) into (A 1)–(A 2) and collecting the terms proportional to $f_c(z)\mathrm{e}^{\mathrm{i}(\theta-t/4)}$, we have the second-order inhomogeneous equations:

$$L_1\begin{pmatrix}a_1^{(2)}\\b_1^{(2)}\\c_1^{(2)}\end{pmatrix} = i\begin{pmatrix}\bar{A}B\left[-\dfrac{\lambda_c I'_1}{4I_1}+\dfrac{\lambda_c K'_1}{4K_1}\right]\\ \bar{A}B\left[-\dfrac{\lambda_c^2 I''_1}{4I_1}+\dfrac{\lambda_c^2 K''_1}{4K_1}\right]\\ -\mathrm{i}\dfrac{\mathrm{d}A}{\mathrm{d}t}-\bar{A}B\left[\dfrac{\lambda_c I'_1}{4I_1}+\dfrac{1}{4}\right]\end{pmatrix}. \tag{A 5}$$

Here, the superscript (2) denotes the order of quantities and the subscript 1 denotes the azimuthal wavenumber $m = 1$. The solvability condition of (A 5) is given as

$$\left(\frac{\lambda_c K'_1}{4K_1}\quad -\frac{1}{4}\quad 1\right)\begin{pmatrix}\bar{A}B\left[-\dfrac{\lambda_c I'_1}{4I_1}+\dfrac{\lambda_c K'_1}{4K_1}\right]\\ \bar{A}B\left[-\dfrac{\lambda_c^2 I''_1}{4I_1}+\dfrac{\lambda_c^2 K''_1}{4K_1}\right]\\ -\mathrm{i}\dfrac{\mathrm{d}A}{\mathrm{d}t}-\bar{A}B\left[\dfrac{\lambda_c I'_1}{4I_1}+\dfrac{1}{4}\right]\end{pmatrix} = 0, \tag{A 6}$$

which leads to (32*a*) with (33). Similarly, collecting the terms proportional to $\mathrm{e}^{2\mathrm{i}(\theta-t/4)}$, we have

$$L_2\begin{pmatrix}a_2^{(2)}\\b_2^{(2)}\\c_2^{(2)}\end{pmatrix} = \mathrm{i}\begin{pmatrix}A^2\gamma\left[\dfrac{1}{2}-\dfrac{\lambda_c I'_1}{4I_1}+\dfrac{\lambda_c K'_1}{4K_1}\right]\\ A^2\gamma\left[-\dfrac{1}{2}-\dfrac{\lambda_c^2 I''_1}{4I_1}+\dfrac{\lambda_c^2 K''_1}{4K_1}\right]\\ -\mathrm{i}\dfrac{\mathrm{d}B}{\mathrm{d}t}+A^2\gamma\left[-\dfrac{\lambda_c I'_1}{2I_1}+\dfrac{1}{4}\right]\end{pmatrix}, \tag{A 7}$$

where the coefficient γ represents the coupling coefficient between $f_c^2(z)$ and the barotropic mode:

$$\gamma = \int_{z_b}^{z_t} \rho_s f_c^2(z)\,\mathrm{d}z \Big/ \int_{z_b}^{z_t} \rho_s\,\mathrm{d}z.$$

The solvability condition of (A 7) is given (taking the limit $\lambda \to 0$ in (A 4)) as

$$(2,1,-2)\begin{pmatrix} A^2\gamma\left[\frac{1}{2}-\frac{\lambda_c I_1'}{4I_1}+\frac{\lambda_c K_1'}{4K_1}\right] \\ A^2\gamma\left[-\frac{1}{2}-\frac{\lambda_c^2 I_1''}{4I_1}+\frac{\lambda_c^2 K_1''}{4K_1}\right] \\ -\mathrm{i}\frac{\mathrm{d}B}{\mathrm{d}t}+A^2\gamma\left[-\frac{\lambda_c I_1'}{2I_1}+\frac{1}{4}\right] \end{pmatrix} = 0, \tag{A 8}$$

which yields (32*b*) with (34).

REFERENCES

ABRAMOWITZ, M. & STEGUN, I. A. 1972 *Handbook of Mathematical Functions*. Natl Bur. Stand./Dover.

BENJAMIN, T. B. & FEIR, J. E. 1967 The disintegration of wave trains on deep water. *J. Fluid Mech.* **27**, 417–430.

BLANCH, G. 1966 Numerical aspects of Mathieu eigenvalues. *Rend. Circ. Mat. Palermo* (2) **15**, 51–97.

CARTON, X. J. & MCWILLIAMS, J. C. 1989 Barotropic and baroclinic instabilities of axisymmetric vortices in a quasi-geostrophic model. In *Mesoscale/Synoptic Coherent Structures in Geophysical Turbulence* (ed. J. C. J. Nihoul & B. M. Jamart), pp. 225–244. Elsevier.

CLEMM, D. S. 1969 Algorithm 352: Characteristic values and associated solutions of Mathieu's differential equation. *Commun. Assoc. Computing Machinery* **12**, 399–407.

CRAIK, A. D. D. 1985 *Wave Interactions and Fluid Flows*. Cambridge University Press.

DRITSCHEL, D. G. 1988*a* Nonlinear stability bounds for inviscid, two-dimensional, parallel or circular flows with monotonic vorticity, and the analogous three-dimensional quasi-geostrophic flows. *J. Fluid Mech.* **191**, 575–581.

DRITSCHEL, D. G. 1988*b* The repeated filamentation of two-dimensional vorticity interfaces. *J. Fluid Mech.* **194**, 511–547.

DRITSCHEL, D. G. 1990 The stability of elliptical vortices in an external straining flow. *J. Fluid Mech.* **210**, 223–261.

FLIERL, G. R. 1988 On the instability of geostrophic vortices. *J. Fluid Mech.* **197**, 349–388.

GENT, P. R. & MCWILLIAMS, J. C. 1986 The instability of circular vortices. *Geophys. Astrophys. Fluid Dyn.* **35**, 209–233.

KIDA, S. 1981 Motion of an elliptic vortex in a uniform shear flow. *J. Phys. Soc. Japan* **50**, 3517–3520.

KLOOSTERZIEL, R. C. & CARNEVALE, G. F. 1992 Formal stability of circular vortices. *J. Fluid Mech.* **242**, 249–278.

LOVE, A. E. H. 1893 On the stability of certain vortex motions. *Proc. Lond. Math. Soc.* **25**, 18–42.

MCWILLIAMS, J. C. 1989 Statistical properties of decaying geostrophic turbulence. *J. Fluid Mech.* **198**, 199–230.

MCWILLIAMS, J. C. 1990 The vortices of geostrophic turbulence. *J. Fluid Mech.* **219**, 387–404.

MEACHAM, S. P. 1992 Quasigeostrophic, ellipsoidal vortices in a stratified fluid. *Dyn. Atmos. Oceans* **16**, 189–223.

MOORE, D. W. & SAFFMAN, P. G. 1971 Structure of a line vortex in an imposed strain. In *Aircraft Wake Turbulence* (ed. J. Olsen, A. Goldburg & N. Rogers), pp. 339–354. Plenum.

MOORE, D. W. & SAFFMAN, P. G. 1975 The instability of a straight vortex filament in a strain field. *Proc. R. Soc. Lond.* A **346**, 413–425.

PEDLOSKY, J. 1979 *Geophysical Fluid Dynamics.* Springer.

ROBINSON, A. C. & SAFFMAN, P. G. 1984 Three-dimensional stability of an elliptical vortex in a straining field. *J. Fluid Mech.* **142**, 451–466.

SALE, A. H. J. 1970 Remark on algorithm 352 [S22]; Characteristic values and associated solutions of Mathieu's differential equation. *Commun Assoc. Computing Machinery* **13**, 750.

TSAI, C.-Y. & WIDNALL, S. E. 1976 The stability of short waves on a straight vortex filament in a weak externally imposed strain field. *J. Fluid Mech.* **73**, 721–733.

WIDNALL, S. E., BLISS, D. B. & TSAI, C.-Y. 1974 The instability of short waves on a vortex ring. *J. Fluid Mech.* **66**, 35–47.